

Scaling metabolism from organisms to ecosystems

Brian J. Enquist*†, Evan P. Economo*, Travis E. Huxman*, Andrew P. Allen‡, Danielle D. Ignace* & James F. Gillooly‡

* Department of Ecology and Evolutionary Biology, University of Arizona, Tucson, Arizona 85721, USA

† Center for Applied Biodiversity Science, 1919 M. Street, NW, Suite 600, Washington DC 20036, USA

‡ Department of Biology, University of New Mexico, Albuquerque, New Mexico 87131, USA

Understanding energy and material fluxes through ecosystems is central to many questions in global change biology and ecology^{1–11}. Ecosystem respiration is a critical component of the carbon cycle^{1,5–7} and might be important in regulating biosphere response to global climate change^{1–3}. Here we derive a general model of ecosystem respiration based on the kinetics of metabolic reactions^{11–13} and the scaling of resource use by individual organisms^{14,15}. The model predicts that fluxes of CO₂ and energy are invariant of ecosystem biomass, but are strongly influenced by temperature, variation in cellular metabolism and rates of supply of limiting resources (water and/or nutrients). Variation in ecosystem respiration within sites, as calculated from a network of CO₂ flux towers^{5,7}, provides robust support for the model's predictions. However, data indicate that variation in annual flux between sites is not strongly dependent on average site temperature or latitude. This presents an interesting paradox with regard to the expected temperature dependence. Nevertheless, our model provides a basis for quantitatively understanding energy and material flux between the atmosphere and biosphere.

Our ability to predict variation in ecosystem processes is currently limited by our ability to mechanistically link biological processes across both spatial and temporal scales^{4,8–10}. One promising approach is to focus on how biotic and abiotic factors regulate metabolic rates of individuals, which combine to determine ecosystem flux rates. Metabolism is the fundamental process dictating material and energy fluxes through organisms^{10–18}. Recent work^{11–14,16} shows that most variation in the metabolic rates of individuals, B_i , can be quantified on the basis of the combined effects of two variables, body size, M_i , and absolute temperature, T in kelvins (k), using the general model for metabolic scaling:

$$B_i = b_0 e^{-E/kT} M_i^{3/4} \quad (1)$$

where b_0 is a normalization constant independent of body size and temperature. The 3/4 power scaling exponent reflects the constraints on resource supply to individual cells through fractal-like distribution networks¹¹. The Boltzmann factor, $e^{-E/kT}$, describes the temperature-dependence of metabolic rate¹², where E is the average activation energy of metabolism (~ 0.6 eV; see ref. 12) and k is Boltzmann's constant (8.62×10^{-5} eV K⁻¹). Previous work indicates that the normalization constant, b_0 , and the activation energy, E , are approximately constant for plants and microbes^{12,13}, the two groups that comprise most of the biomass in terrestrial ecosystems.

Here we build on the general model (equation (1)) to account for variation in rates of ecosystem respiration at sites across the globe. We assume that, at a given site, organisms grow and fill physical space so that the rate of resource use by all individuals, Q_{tot} , is proportional to R , the approximate rate of limiting resource supply (such as water and/or nutrients) when evaluated per unit area per unit time (see ref 10). The respiration rate of an ecosystem, B_e , is equal to the sum of the individual metabolic rates, B_i , for all

Box 1

A general model for scaling biochemical kinetics from organisms to ecosystems

The total ecosystem metabolic flux per unit area, B_e , is influenced by the number of organisms of a given size, M_i , and their respective metabolic rates, B_i . To account for the allometric dependence of B_e , we conduct the summation of B_i across n discrete body size classes, indexed by j , from the smallest sizes (m_1) to the largest sizes (m_n). Here m_j is the average mass within a given arbitrary bin or size class used to resolve the size distribution. Specifically, the whole-system metabolism is the summation of the average metabolic rate of all organisms within each size class, B_j , and their associated total population density, N_j , so that

$$B_e \approx \sum_{j=1}^n [(B_j)(N_j)]$$

Here the total biomass contained within the j th bin is given by $M_j^{\text{tot}} = m_j N_j$ and the density of individuals per bin is given by $N_j = M_j^{\text{tot}}/m_j$. Thus, from equation (1) we have

$$B_e = \left[\sum_{j=1}^n (e^{-E/kT} b_0 m_j^{3/4})(N_j) \right] = e^{-E/kT} b_0 \left[\sum_{j=1}^n (m_j^{3/4}) \left(\frac{M_j^{\text{tot}}}{m_j} \right) \right] \quad (1.1)$$

Equation (1.1) can then be simplified as

$$Q_{\text{tot}} \propto B_e = e^{-E/kT} b_0 \left[\sum_{j=1}^n (m_j^{-1/4})(M_j^{\text{tot}}) \right] \quad (1.2)$$

where the $-1/4$ power accounts for the allometric scaling of organismal mass-specific metabolism. The proportion (α_j) of the total standing ecosystem biomass, M_e^{tot} , that resides within each mass bin, m_j , is $\alpha_j \equiv m_j N_j / M_e^{\text{tot}}$ so that $M_j^{\text{tot}} = \alpha_j M_e^{\text{tot}}$, where $0 < \alpha_j \leq 1$ and the sum

$$\sum_{j=1}^n \alpha_j = 1$$

For a given M_e^{tot} , the value of α_j is influenced by the width of the bin used to resolve the size distribution ($m_j - m_{j-1}$), the density of individuals per bin (N_j) and the total number of bins (n) relative to the total standing biomass, M_e^{tot} .

Simplifying gives the general form of the ecosystem respiration equation,

$$Q_{\text{tot}} \propto B_e = e^{-E/kT} b_0 \left[M_e^{\text{tot}} \left(\sum_{j=1}^n \alpha_j m_j^{-1/4} \right) \right] \quad (1.3)$$

where the term

$$\left(\sum_{j=1}^n \alpha_j m_j^{-1/4} \right)$$

represents the allometric dependence as reflected in the community size distribution. Empirical data and allometric theory show that $Q_{\text{tot}} \approx B_e \approx R$ is independent of the standing biomass, M_e^{tot} (ref. 10). This invariance, or the energetic equivalence rule (EER)^{10,17}, predicts that within a given environment, if R is constant, the value of B_e is independent of M_e^{tot} . Thus, the value of

$$\left[M_e^{\text{tot}} \left(\sum_{j=1}^n \alpha_j m_j^{-1/4} \right) \right]$$

(henceforth shown as C) is constrained to be proportional to resource availability, so that $C \propto R$. Therefore, according to the EER, if R varies between environments (and T , E and b_0 are constant) our model predicts that B_e and Q_{tot} will vary accordingly as $Q_{\text{tot}} \approx B_e \approx C \propto R$. As a result, variation in R must then influence the nature of the size distribution within a given ecosystem through linked or separate variation in M_e^{tot} , the density of individuals of a given size ($m_j N_j$) and the maximum (m_n) and/or minimum (m_1) sizes of organisms.

We can now rearrange equation (1.3) into the following general form:

$$\ln(Q_{\text{tot}}) \propto \ln(B_e) = \frac{-E}{1,000k} \left(\frac{1,000}{T} \right) + \ln[(b_0)(C)] \quad (1.4)$$

where, again, $C \propto R$. Equation (1.4) is similar in form to an Arrhenius plot for calculating activation energies for biochemical reactions^{19,20,32,33}. Here, however, values of E represent the activation energy for metabolism across plants, animals and microbes found within a given assemblage (see Methods and ref. 12).

organisms in that system:

$$R \propto Q_{\text{tot}} \propto B_e = \sum_i B_i \quad (2)$$

This expression can be simplified by using the derivation in Box 1 to yield the following expression:

$$\ln(R) \propto \ln(Q_{\text{tot}}) \propto \ln(B_e) = \frac{-E}{1,000k} \left(\frac{1,000}{T} \right) + \ln[(b_0)(C)] \quad (3)$$

Equation (3) provides a general function for the scaling of ecosystem respiration and yields three important predictions. First, for a given ecosystem, plotting $\ln(B_e)$ against $(1,000/T)$ should yield a general linear relationship describing the dependence of ecosystem respiration on temperature. Second, the slope of this relationship, across diverse ecosystems, should be $-E/1,000k \approx -7.5 \text{ K}$, reflecting the fundamental importance of the activation energy of metabolism in constraining whole-ecosystem respiration (see Methods). Last, because of the energetic equivalence rule (EER; see Box 1), ecosystem respiration should be independent of the total standing biomass across sites if rates of resource supply are held constant (for example, grasslands and forests can have similar values of B_e). Equation (3) also shows the functional

dependence of the intercept on b_0 and C , which characterize the intensity of cellular metabolism, and the size abundance distribution of organisms, respectively (Box 1). Note that the limiting resource supply rate, R , might influence ecosystem respiration through its effects on one or both of these variables.

We evaluated these predictions by compiling nightly ecosystem CO_2 flux rates, B_e , throughout the year from flux towers across the globe. Data were assembled from FLUXNET^{5,7} (see Methods and Supplementary Table 1). Plotting $\ln(B_e)$ (in W ha^{-1}) against the reciprocal of absolute temperature ($1,000/T$) for 19 eddy covariance flux-tower sites in both Europe and North America provides robust support for the model's predictions (Fig. 1; Supplementary Table 1). First, at all sites, the natural logarithm of ecosystem respiration rate is linearly related to the reciprocal of absolute temperature. Second, the average of the observed slopes across ecosystems for all years ($\bar{x} = -7.17$, 95% confidence interval -6.53 to -7.81 , $n = 45$) is indistinguishable from the value predicted from the temperature dependence of individual metabolism (-7.79 ± 1.63) (ref. 12). Furthermore, the slopes all fall within the range expected from the measured activation energies of metabolic reactions (see Methods). Third, analysis of the 95% confidence intervals indicates a strong overlap in the values of the slopes and annual night-time CO_2 fluxes

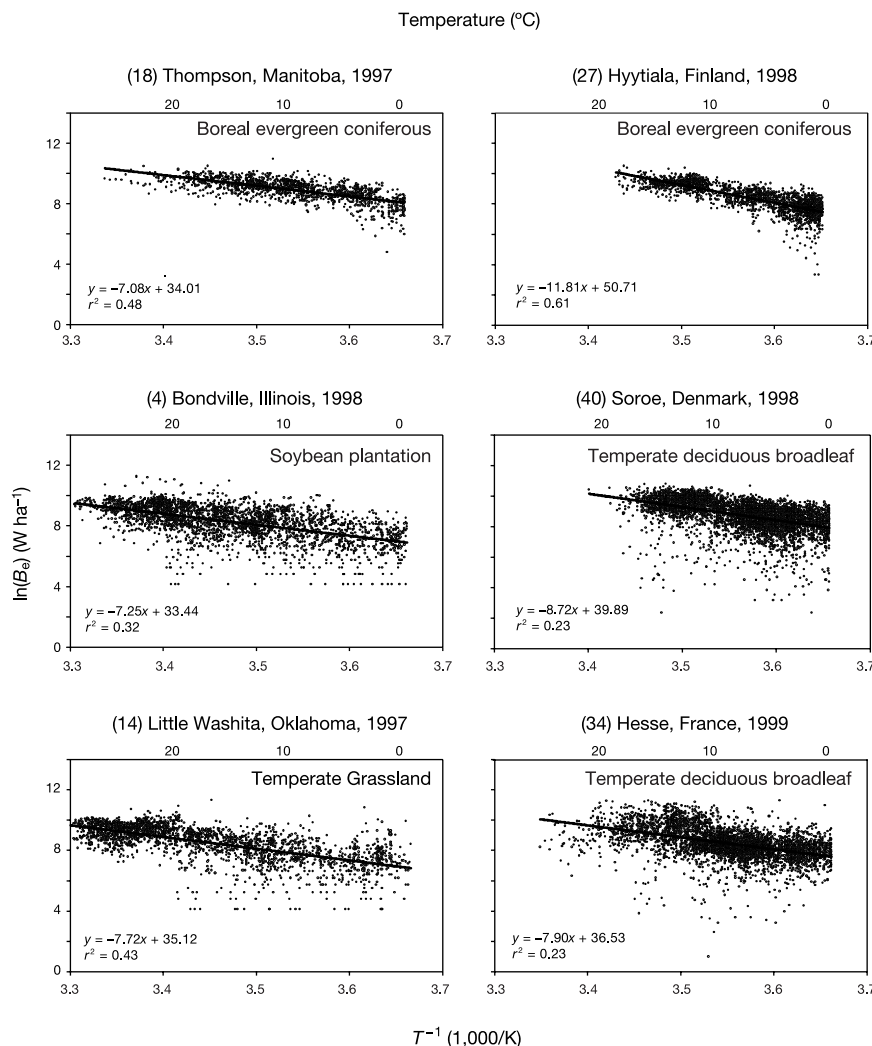


Figure 1 A plot of night-time ecosystem flux, $\ln(B_e)$, against the reciprocal of absolute temperature for 30-min average samples throughout the year for six representative eddy covariance flux-tower sites. The slope of the temperature response reflects the activation

energy of this rate process. Both the range and the average of the slopes across ecosystems are statistically indistinguishable from predictions of the model. Numbers on the top portion of each graph refer to temperature in $^{\circ}\text{C}$.

across all ecosystems, which differ in standing biomass and floristic composition, and which include 14 forests, 2 grasslands, 2 desert sites and an agricultural site (Figs 2a and 3; Supplementary Table 1). The similarity of the slopes of these relationships across sites comprising different taxa (for example, Europe versus America), plant functional types (conifers versus angiosperms), photosynthetic pathways (C_3 versus C_4) and diversity (low latitude versus high latitude) provides strong evidence that ecosystem flux is constrained by the activation energy of individual metabolism.

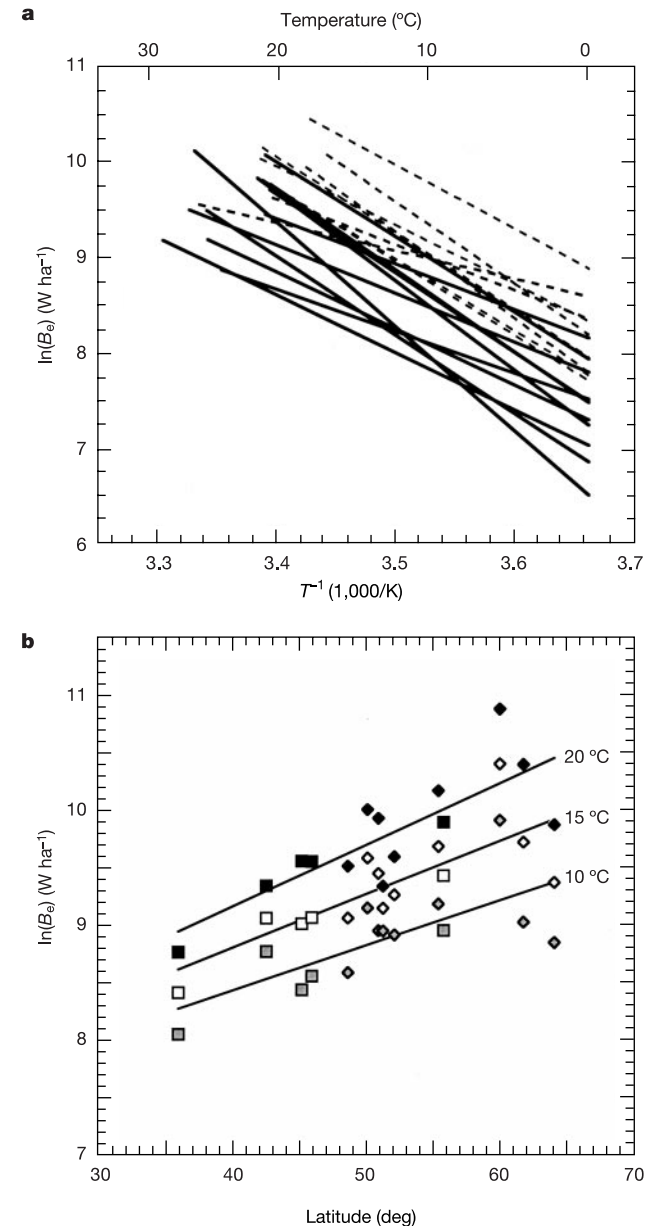


Figure 2 Summary of variability in the temperature and flux function across sites. These figures indicate an increase in the temperature-normalized instantaneous flux with increasing latitude. **a**, Fitted night-time flux functions for all 19 sites in North America (solid lines) and Europe (dashed lines). **b**, Plot of the average ecosystem flux intercept for each forest site normalized at three temperatures (20, 15 and 10 °C; that is, $\ln(B_e(20^\circ\text{C}))$) against latitude shows a significant positive relationship (diamonds, Europe; squares, North America). All forest sites at 20 °C: $r^2 = 0.651$, $n = 14$, $P = 0.000487$; European sites at 20 °C: $r^2 = 0.361$, $n = 9$, $P = 0.087$; North American sites at 20 °C: $r^2 = 0.915$, $n = 5$, $P = 0.0108$. Black, white and grey symbols represent flux values normalized at 20, 15 and 10 °C respectively.

The empirical fits to the predicted flux functions reveal a wide range of intercept values for European and North American sites (see Fig. 2a). This variation might be due to a systematic change in the temperature-corrected ecosystem respiration rate with latitude². Applying analysis of covariance (ANCOVA) to the entire flux data set, we find a significant overall effect of temperature on ecosystem flux (type III SS: d.f. = 1, $F = 20,888$, $P < 0.0001$). In addition, we find significant differences between sites and years in the intercepts (d.f. = 44, $F = 743.9$, $P < 0.0001$) and slopes (type III SS: d.f. = 44, $F = 63.9$, $P < 0.0001$). Holding the slope constant for all sites (pooled ANCOVA slope of -7.40) still reveals significant differences in the fitted intercepts between sites (type III SS: d.f. = 44, $F = 725.52$, $P < 0.0001$). Such differences might also reflect differences in resource supply (R) between sites. Restricting the analysis to forest sites only, where values of M_e^{tot} are similar (see also ref. 10), still reveals differences in fitted intercepts across sites (ANCOVA constant slopes model type III SS: d.f. = 36, $F = 522.72$, $P < 0.0001$).

The within-site average fitted intercepts (from the fixed-slopes model from the ANCOVA) for all sites and for forest sites are positively correlated with latitude (all sites: $n = 19$, $r^2 = 0.61$, $F = 27.07$, $P = 0.0001$; forest sites: $n = 14$, $r^2 = 0.424$, $F = 8.83$, $P = 0.012$). Thus, geographic variation in the fitted intercepts indicates that high-latitude ecosystems are characterized by an approximately 3–6-fold increase in CO_2 flux at a given temperature when compared with lower-latitude sites. For each forest site, plotting the temperature-normalized flux rates at three different temperatures (20, 15 and 10 °C) shows a significant increase with latitude (Fig. 2b). Perhaps as a consequence, the annual night-time CO_2 flux does not vary significantly with average annual temperature or latitude (Fig. 3; $P > 0.10$; see also ref. 1). There are several possible explanations for this pattern. These include latitudinal gradients in resource availability (R) or community structure (related to C), lag effects from daytime respiration, and calibration of towers across sites. These results are also qualitatively consistent with results indicating that individuals in colder climates adjust

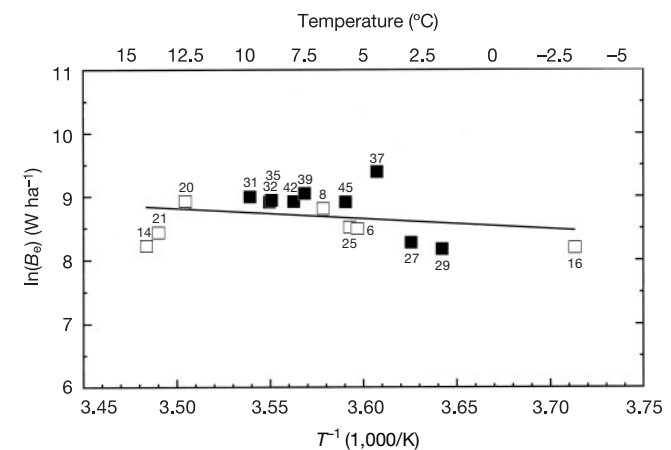


Figure 3 Relationship between the annual night-time CO_2 flux (average rate per second) and the average annual night-time temperature for both North American (open symbols) and European sites (solid symbols). Sites include 16 forests and 2 grasslands (symbols numbered 14 and 20). Note that annual night-time respiration does not vary significantly with temperature across sites (for forest ecosystems, $r^2 = 0.21$, s.e.m. = 0.337, $n = 14$, slope = -3.13 , intercept = 19.95, $P = 0.101$; see also table 1 in ref. 1). Further, as outlined by our model, ecosystem flux is not constrained by standing biomass because our grassland sites, and the agricultural site, have similar flux rates to those of the forest sites. Numbers beside each symbol refer to site numbers listed in Supplementary Table 1.

their metabolic rates (in other words, they increase b_0) to compensate for shorter growing seasons^{19–24}. The paradox illustrated here and in other recent studies^{2,9,21,22} highlights the need for further investigation of the linkages between organismal and ecosystem attributes. It also casts doubt on studies of climate change that extrapolate within-site temperature responses of organisms to regional or global scales (see refs 2, 9).

Studies of atmospheric $\delta^{13}\text{C}$ distributions strongly imply that the terrestrial biosphere contributes to inter-annual variability in global CO_2 (refs 25, 26). Our model provides a mechanistic basis for understanding how variation in resource availability, temperature and the size distribution of organisms (namely R , T and C) influence the flux of energy and materials (namely B_e , Q_{tot}) through ecological systems. The model yields many testable predictions^{10–14}. It highlights the similarity of the temperature dependence of whole-system flux, across sites comprising differing taxa, plant functional types, physiological pathways and diversity. It also explains how other prominent features of ecosystems such as standing biomass (M_e^{tot}), floristic composition and diversity might not influence ecosystem flux. Residual variation not accounted for by the model emphasizes the importance of other biotic and abiotic factors in determining ecosystem respiration (such as variability in resource availability, phenology, seasonality and life-history variation). Nevertheless, our model provides a framework for the assessment and quantitative integration of additional biotic and abiotic influences on CO_2 flux. Thus, a focus on the fundamental importance of metabolism offers a basis on which to integrate cellular, physiological and ecological attributes of ecological systems. □

Methods

We evaluated our model predictions with data from a network of micrometeorological sites that measure CO_2 , water vapour and energy exchange between the biosphere and atmosphere using the eddy covariance technique (FLUXNET⁹). FLUXNET is a unique and powerful diagnostic tool for assessing local and global scale variation in ecosystem production, respiration and net carbon exchange¹. FLUXNET consists of up to 140 sites operating on a semi-continuous basis. However, only 19 sites, with 45 site-years, provided robust continuous intra-annual measurements with multiple year records and sufficient temperature ranges. FLUXNET data have been standardized and distributed²⁷. Sites were selected from a diverse group of ecosystems, including temperate conifer and broadleaved (deciduous and evergreen) forests, boreal forest, cropland and grasslands. Together, these sites span two continents (Europe and North America) with a broad latitudinal range ($\sim 65^\circ\text{N}$ to 30°N). We also added two (non-FLUXNET) low-productivity sites from the Sonoran and Mojave Desert operated by the authors of this study. These sites each consist of 5 months' worth of continuous flux during the winter and spring seasons in 2002.

The eddy covariance technique measures net carbon and water fluxes between the biosphere and atmosphere from relatively large areas (longitudinal lengths of footprints between 100 and 2,000 m) with minimal disturbance to the system, for short and long timescales (hours, days, seasons and years; see ref. 28). Measurements of net ecosystem CO_2 exchange (NEE) during daylight hours are a function of plant photosynthesis along with both autotrophic and heterotrophic respiration. It is currently not possible to disentangle rates of respiration and photosynthesis continuously during the day (see ref. 5), but nightly values of CO_2 exchange approximate a biological ecosystem flux, or total respiration. Nightly flux values therefore provide a unique measurement of whole-system metabolism or energy flux. Here, night time is defined as the time during which the measured photosynthetically active radiation at each site is zero. To standardize ecosystem respiration, B_e , in units of metabolic energy we then converted nightly values of CO_2 flux into energy flux (W ha^{-1}). Because ATP and CO_2 are both end products of respiration, the conversion is accomplished with their stoichiometry and an estimated value of available energy in quantities of ATP ($51 \text{ kJ mol}^{-1} \text{ ATP}$) \times ($32 \text{ mol ATP/6 mol CO}_2$) = $0.272 \text{ J } \mu\text{mol}^{-1} \text{ CO}_2$ (ref. 29). FLUXNET reports NEE in units of $\mu\text{mol m}^{-2} \text{ s}^{-1}$, where $(\text{NEE}) \times (0.272 \text{ J } \mu\text{mol}^{-1} \text{ CO}_2) \times (10,000 \text{ m}^2 \text{ ha}^{-1}) = B_e$ in $\text{J}^{-1} \text{ ha}^{-1} \text{ s}^{-1}$. To parameterize equation (3) we used empirical values of biological activation energies, which vary between 0.2 and 1.2 eV, with an average of $\sim 0.6 \text{ eV}$ (refs 12, 30, 31). Transformed values of ecosystem flux were analysed with Model I regression analysis, because significant measurement error is likely to exist primarily on measures of CO_2 flux. Statistical analysis of variation in the fitted flux intercepts and slopes across sites were computed in S+ by using ANCOVA.

Studies of activation energies, E , for the respiratory complex across differing plant and animal species show little variation^{12,13,19}. Substituting the average biological activation energies predicts that the slope, $-E/1,000k$, where k is Boltzmann's constant, of the ecosystem respiration function should have a universal value of about -7.4 (ref. 12) but can range between -2 and -11 . Further, calculated activation energies for whole-organismal metabolism for both animals and plants¹² reveal a similar value of -7.79 (95% confidence interval -6.16 to -9.42).

Received 23 September 2002; accepted 20 March 2003; doi:10.1038/nature01671.

1. Valentini, R. *et al.* Respiration as the main determinant of carbon balance in European forests. *Nature* **404**, 861–865 (2000).
2. Giardina, C. P. & Ryan, M. G. Evidence that decomposition rates of organic carbon in mineral soil do not vary with temperature. *Nature* **404**, 858–861 (2000).
3. Huxman, T. E. *et al.* Temperature as a control over ecosystem CO_2 fluxes in a high elevation subalpine forest. *Oecologia* **134**, 537–546 (2003).
4. Rosenzweig, M. L. *Species Diversity in Space and Time* (Cambridge Univ. Press, 1995).
5. Baldocchi, D. *et al.* FLUXNET: A new tool to study the temporal and spatial variability of ecosystem-scale carbon dioxide, water vapor, and energy flux densities. *Bull. Am. Meteorol. Soc.* **82**, 2415–2434 (2001).
6. Law, B. E. Environmental controls over carbon dioxide and water vapor exchange of terrestrial vegetation. *Agric. Forest Meteorol.* **113**, 97–120 (2002).
7. Running, S. W. *et al.* A global terrestrial monitoring network, scaling tower fluxes with ecosystem modeling and EOS satellite data. *Remote Sens. Environ.* **70**, 108–127 (1999).
8. Schulze, E. D., Kelliher, F. M., Korner, C., Lloyd, J. & Leuning, R. Relationships among maximal stomatal conductance, carbon assimilation rate, and plant nitrogen nutrition: A global ecology scaling exercise. *Annu. Rev. Ecol. Syst.* **25**, 629–660 (1994).
9. Luo, Y., Wan, S., Hui, W. & Wallace, L. L. Acclimatization of soil respiration to warming in a tall grass prairie. *Nature* **413**, 622–625 (2001).
10. Enquist, B. J. & Niklas, K. J. Invariant scaling relations across tree-dominated communities. *Nature* **410**, 655–660 (2001).
11. West, G. B., Brown, J. H. & Enquist, B. J. A general model for the origin of allometric scaling laws in biology. *Science* **276**, 122–126 (1997).
12. Gillooly, J. F., Brown, J. H., West, G. B., Savage, V. M. & Charnov, E. L. Effects of size and temperature on metabolic rate. *Science* **293**, 2248–2251 (2001).
13. Gillooly, J. F. *et al.* Effects of size and temperature on developmental time. *Nature* **417**, 70–73 (2002).
14. Niklas, K. J. & Enquist, B. J. Invariant scaling relationships for interspecific plant biomass production rates and body size. *Proc. Natl Acad. Sci. USA* **98**, 2922–2927 (2001).
15. Hemmingsen, A. M. Energy metabolism as related to body size and respiratory surfaces, and its evolution. *Rep. Steno Mem. Hosp. Nord. Insulin Lab.* **9**, 7–95 (1960).
16. West, G. B., Woodruff, W. H. & Brown, J. H. Allometric scaling of metabolic rate from molecules and mitochondria to cells and mammals. *Proc. Natl Acad. Sci. USA* **99** (suppl. 1), 2473–2478 (2002).
17. Damuth, J. Population density and body size in mammals. *Nature* **290**, 699–700 (1981).
18. Enquist, B. J. in *Macroecology: Concepts and Consequences* (eds Blackburn, T. & Gaston, K.) (Oxford Univ. Press, in the press).
19. Raison, J. K. & Chapman, E. A. Membrane phase changes in chilling-sensitivity *Vigna radiata* and their significance to growth. *Aust. J. Plant Physiol.* **3**, 291–299 (1976).
20. Pearcy, R. W. Acclimation of photosynthetic and respiratory carbon dioxide exchange to growth temperature and *Atriplex lentiformis* (Torr.) Wats. *Plant Physiol.* **59**, 795–799 (1977).
21. Conover, D. O. & Schultz, E. T. Phenotypic similarity and the evolutionary significance of countergradient selection. *Trends Ecol. Evol.* **10**, 248–252 (1995).
22. Mooney, H. A. & Billings, W. D. Comparative physiological ecology of arctic and alpine populations of *Oxyria digyna*. *Ecol. Monogr.* **31**, 1–29 (1961).
23. Lovegrove, B. G. The zoogeography of mammalian basal metabolic rate. *Am. Nat.* **156**, 201–219 (2000).
24. Jordan, C. F. A world pattern of plant energetics. *Am. Sci.* **59**, 425–433 (1971).
25. Ciais, P., Tans, P. P., Trolier, M., White, J. W. C. & Francy, R. J. A large North Hemisphere terrestrial CO_2 sink indicated by the $^{13}\text{C}/^{12}\text{C}$ ratio of atmospheric CO_2 . *Science* **269**, 1098–1102 (1995).
26. Keeling, C. D. & Whorf, T. P. *Trends '93: A Compendium of Data on Global Change* Oak Ridge National Laboratory Report ORNL/CDIAC-65 16–26, (1994).
27. Falge, *et al.* Gap filling strategies for defensible annual sums of net ecosystem exchange. *Agric. Forest Meteorol.* **107**, 43–69 (2001).
28. Baldocchi, D. D., Hicks, B. B. & Meyers, T. P. Measuring biosphere-atmosphere exchanges of biologically related gases with micrometeorological methods. *Ecology* **69**, 1331–1340 (1988).
29. Nelson, D. L. & Cox, M. M. *Lehninger Principles of Biochemistry* 3rd edn (Worth Publishing, New York, 2000).
30. Vetter, R. A. H. Ecophysiological studies on citrate synthase. 1. Enzyme regulation of selected crustaceans with regard to temperature adaptation. *J. Comp. Physiol. B* **165**, 46–55 (1995).
31. Raven, J. A. & Geider, R. J. Temperature and algal growth. *New Phytol.* **110**, 441–461 (1988).
32. Nobel, P. S. *Physicochemical and Environmental Plant Physiology* (Academic, New York, 1999).
33. Earnshaw, M. J. Arrhenius plots of root respiration in some arctic plants. *Arctic Alpine Res.* **13**, 425–430 (1981).

Supplementary Information accompanies the paper on www.nature.com/nature.

Acknowledgements We thank D. Baldocchi for assistance with accessing FLUXNET data; the contributors of FLUXNET for their support of this project; and M. Weiser, D. Kerkhoff, N. Phillips, J. Harte, K. J. Niklas, S. Cowing, J. Williams and J. H. Brown for providing assistance and/or comments on earlier drafts. B.J.E. was supported by an NSF CAREER fellowship and a Center for Applied Biodiversity, Conservation International Fellowship, a LANL grant, and the University of Arizona. T.E.H. was supported by an award from IALC and the University of Arizona. B.J.E. and T.E.H. acknowledge support from the Institute for the Study of Planet Earth at the University of Arizona. J.F.G. acknowledges support from the Thaw Charitable Trust and the Packard Foundation. A.P.A. acknowledges support from NSF.

Competing interests statement The authors declare that they have no competing financial interests.

Correspondence and requests for materials should be addressed to B.J.E. (benquist@u.arizona.edu).